Cellulose
https://doi.org/10.1007/s10570-025-06785-4

ORIGINAL RESEARCH

# Residual lignin affects production and properties of TEMPO-oxidized cellulose nanofibrils from partially delignified sugarcane bagasse

**Eupidio Scopel · Lidiane O. Pinto · Camila A. Rezende**

Received: 11 April 2025 / Accepted: 21 September 2025


**Abstract** This study investigated the production of cellulose nanofibrils (CNFs) from partially delignified sugarcane bagasse (SCB), focusing on the effects of residual lignin on TEMPO oxidation and CNF properties. Through a comprehensive assessment of SCB processing into CNFs, we explored the correlations between initial lignin content (15–24 wt%), the amount of NaClO (25–50 mmol/g substrate), and the resulting chemical, morphological, and surface modifications. Regardless of the initial lignin content, oxidizing agent level, or type of mechanical treatment (ultrasonication or microfluidization), CNFs with average lengths of ~ 600–800 nm were obtained. However, in substrates with higher initial lignin content (24 wt%), increasing the NaClO concentration from 25 to 50 mmol/g substrate enhanced fibrillation but reduced the average CNF length from 813 to 665 nm. In contrast, no significant differences in fibrillation were observed when using 25 or 50 mmol NaClO/g substrate in samples with lower initial lignin content (15 wt%). Overall, TEMPO oxidation reduced lignin levels to 5–7.5 wt%, despite substantial differences in the starting materials. Substrates with higher initial lignin content yielded lower amounts of carboxylated groups, likely due to the oxidizing agent being consumed in lignin removal rather than cellulose oxidation. Morphological characterization of the substrates before and after TEMPO oxidation highlighted the critical role of this step in modifying fiber structure, which directly correlated with fibrillation efficiency. Zeta potential and rheological analyses highlighted the potential of CNFs produced from a single-step delignification process for high-value applications such as rheology modifiers, hydrogels, and films.

**Keywords** Nanocellulose · Organosolv · Biorefinery · Lignocellulosic biomass · Lignin-containing cellulose nanofibril

**Supplementary Information** The online version contains supplementary material available at https://doi.org/10.1007/s10570-025-06785-4.

E. Scopel (✉) · L. O. Pinto · C. A. Rezende (✉)
Instituto de Química, Universidade Estadual de Campinas - UNICAMP, Campinas, SP 13083-970, Brazil
e-mail: eupidio.scopel@ubc.ca

C. A. Rezende
e-mail: camilaiq@unicamp.br

L. O. Pinto
e-mail: l136551@dac.unicamp.br

*Present Address:*
E. Scopel
Department of Wood Science, The University of British Columbia, Vancouver, BC V6T 1Z4, Canada

## Introduction

Cellulose nanofibrils (CNFs) are renewable structures derived from natural resources, primarily lignocellulosic biomass, including wood, grasses, and agro-industrial residues (Moon et al. 2011; De France et al.

Published online: 10 October 2025

2017). CNFs exhibit nanometric cross-sections (*ca.* 2–20 nm) and lengths up to micrometer-scale, being flexible and capable of entangling and forming gels at low concentrations (around 1 wt%) (Eichhorn et al. 2010; De France et al. 2017). Thus, CNFs have demonstrated versatility in various applications, including the preparation of hydrogels (Du et al. 2019), aerogels and cryogels (Ferreira et al. 2021), films (Fang et al. 2019), emulsions (Kedzior et al. 2021), and electronic devices (Hoeng et al. 2016). These applications benefit from the unique properties of CNFs, including high aspect ratio, tunable surface chemistry, rheological behavior, and optical and barrier properties (Isogai et al. 2011; Abitbol et al. 2016).

CNF production from lignocellulosic biomasses involves extracting cellulose fibrils, which are embedded in a lignin–hemicellulose matrix in the plant cell wall, commonly using a combination of chemical and mechanical treatments (Himmel et al. 2007; Isogai et al. 2011). Due to the multicomponent and hierarchical nature of biomass, an initial delignification step is commonly applied to remove non-cellulosic components (Isogai et al. 2011; Mariano et al. 2014; de Amorim et al. 2020). After that, chemical modifications, such as oxidation with the radical 2,2,6,6-Tetramethylpiperidine 1-oxyl (TEMPO), are applied prior to mechanical treatments to enhance fibrillation and reduce costs. TEMPO-mediated oxidation is a traditional method applied for CNF production that introduce carboxyl groups onto cellulose surface, improving fiber wettability and electrostatic repulsion during mechanical fibrillation (Saito et al. 2007; Isogai et al. 2011; Rol et al. 2019). In sequence, CNFs can be produced through mechanical fibrillation of TEMPO-oxidized substrates using refiners (Kargupta et al. 2021), grinders (Iwamoto et al. 2007), homogenizers (Wang et al. 2019), microfluidizers (Carneiro Pessan et al. 2023), or ultrasonicators (Scopel et al. 2023).

A key challenge in CNF production is achieving efficient fibrillation while preserving cellulose integrity or yield since harsh delignification can damage fibers and reduce the aspect ratio of the resulting CNFs (Isogai et al. 2011; de Oliveira et al. 2016). Retaining lignin in the substrate prior to surface modification and mechanical disintegration is a promising strategy to avoid excessive damage to cellulose fibers. The so-called lignin-containing cellulose nanofibrils (LCNF) have been recently reported, demonstrating that the presence of residual lignin can impact nanocellulose properties, such as enhanced oxygen barrier in films, antioxidant activity, and UV-light absorption (Imani et al. 2019; Han et al. 2020; Patterson et al. 2023; Almeida et al. 2024). However, retaining lignin usually results in lower fibrillation yields due to the lignin intrinsic function in plant cell wall (Puangsin et al. 2017; Wen et al. 2019). Likewise, TEMPO oxidation notably removes lignin, in addition to the conversion of hydroxy into carboxy groups (Ma et al. 2012), which may be considered when applied to partially delignified substrates.

The understanding of TEMPO oxidation applied to lignin-containing substrates and its influence on CNF properties is particularly relevant for agro-industrial residues, such as sugarcane bagasse (SCB). Recent studies have demonstrated the potential of producing CNFs from SCB through TEMPO oxidation (Pinto et al. 2019; Haroni et al. 2021; Carneiro Pessan et al. 2023). Previous studies have indicated lignin removal as a consequence of TEMPO oxidation in nanocellulose production from thermomechanical pulp from softwood (Okita et al. 2009), jute fibers (Sharma et al. 2025), poplar (Wen et al. 2019), and switchgrass (Sun et al. 2022). However, there is still a lack of understanding of how TEMPO oxidation affects partially delignified SCB. This is particularly relevant considering that TEMPO oxidation applied to highly delignified SCB (lignin content of 3.5 wt%) has been shown to produce cellulose nanocrystals (CNCs) rather than CNFs by increasing the concentration of the oxidizing agent (Pinto et al. 2019). It suggests that TEMPO oxidation step also may alter nanocellulose morphology, which could be potentially surpassed by using less delignified substrates that are less prone to damage during oxidation. It is important to highlight that each biomass responds differently when subjected to the same delignification conditions due to the differences in morphology and chemical composition and these differences must be considered during TEMPO oxidation. Given the abundance of SCB, rationalizing CNF production from this substrate is important for enhancing its value using delignification routes other than the conventional delignification-bleaching sequence (de Oliveira et al. 2016; Pinto et al. 2019; Carneiro Pessan et al. 2023). In addition, it is crucial for tailoring CNF properties since residual lignin can affect charge distribution, fibrillation mechanisms, and efficiency, contributing

to understanding CNF production from a fundamental perspective.

This study investigates the relationship between residual lignin content and TEMPO oxidation levels with the production and properties of CNFs from SCB. Specifically, the goal was not only to produce CNFs but also to understand the fundamental effects of remaining lignin on fiber chemistry, oxidation efficiency, and CNF morphology. Understanding these factors is key to optimizing CNF production from SCB and tailoring its properties for target applications, while also providing a holistic perspective of biomass processing, including the use of lignin as a byproduct. A Design of Experiments (DoE) approach was used to select two conditions for organosolv delignification with aqueous ethanol solutions, producing substrates with different lignin levels. Lignin content, fiber morphology, and surface charge were evaluated to develop efficient CNF production from SCB through a single organosolv delignification step.

## Methodology

### Materials

Sugarcane bagasse was kindly donated by Raízen® (Piracicaba, Brazil). Raw samples were dried in a convection oven (Tecnal, TE-394/3) under 60 °C for 8 h, milled in a knife mill (Arthur H. Thomas Co – Standard model 3) until passing through a 2 mm sieve, and stored in plastic containers. NaBr (99% purity), ethanol (99.5% purity), glacial acetic acid (99.7% purity), NaOH (99% purity), HCl (36.5–38% purity), $H_2SO_4$ (95–98% purity), and silicone oil (350 cps) were purchased from Synth® (Diadema, Brazil); TEMPO (98% purity), acetyl bromide (99% purity), and hydroxylamine-HCl (98% purity) were purchased from Sigma Aldrich®; and NaClO (10–12% purity) was acquired from Êxodo Científica® (Sumaré, Brazil). All reactants were used as received.

### Production of CNFs

#### *Process summary*

The steps involved in CNF production from raw SCB are illustrated in Fig. 1 and include: 1) Delignification;

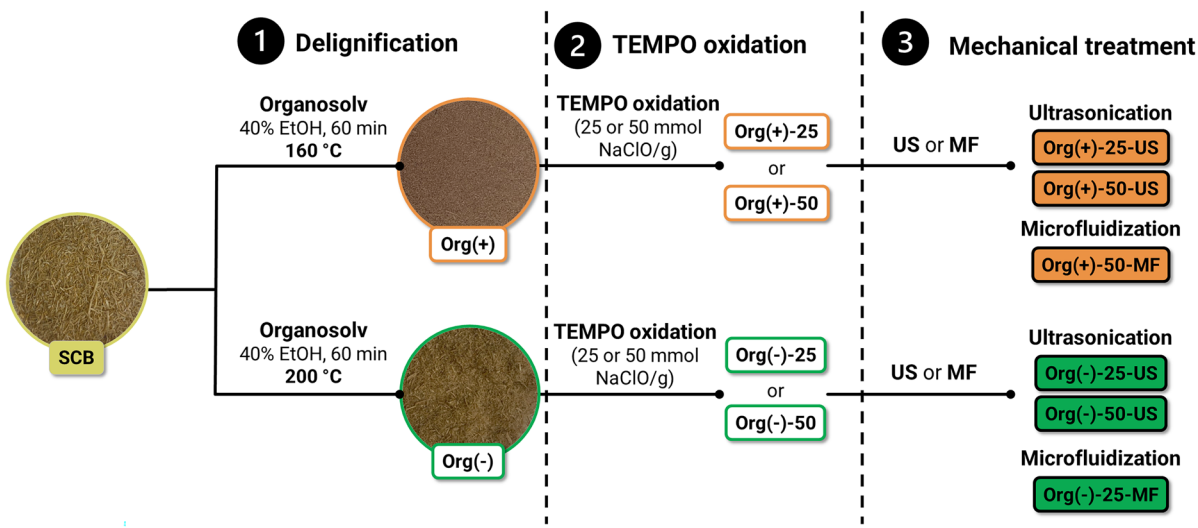


**Fig. 1** Schematic process for CNF preparation from SCB, involving: 1) Delignification by organosolv extraction at two levels, resulting in samples Org(+) and Org(−), where + and— symbols refer to high and low lignin content, respectively; 2) TEMPO oxidation using two levels of NaClO (25 or 50 mmol/g), as indicated by the suffixes 25 and 50, respectively; and 3) Mechanical treatments (ultrasonication or microfluidization), where US and MF represent ultrasonication and microfluidization, respectively

2) TEMPO oxidation; and 3) Mechanical treatment. A detailed description of each step is provided in the following sections.

*Delignification with organosolv extraction*

Partially delignified samples were obtained through organosolv extraction using aqueous ethanol solutions (de Oliveira et al. 2016; Rabelo et al. 2022), as shown in Fig. 1. A $2^3$ Factorial Design (three variables evaluated in two different levels) was used for screening experimental conditions. The studied variables were ethanol concentration (40 or 80% v/v), time (60 or 120 min), and temperature (160 or 200 °C), resulting in 8 experiments and 3 central points (60% v/v ethanol, 90 min, and 180 °C). Cellulose, hemicellulose, lignin, and ash contents for all DoE proposed conditions are presented in Supplementary Information (Section S1, Table S1, and Figure S1). Lignin content was selected as the response in DoE.

Experiments were conducted using 10 g of SCB (dry mass) and 100 mL of the aqueous ethanol solution in a stainless-steel reactor immersed in a silicone oil bath preheated to the target temperature. After the reaction, the system was cooled in an ice bath for 1 h. The solid substrate was filtered through 75 µm nylon sieve, rinsed first with 200 mL of ethanol to prevent lignin reprecipitation onto cellulose fibers, and then with tap water until rinsing water became colorless. The solid substrate was then dried in a convection oven (60 °C, 6 h) and stored for chemical and morphological characterization and CNF production.

Based on DoE, samples with higher lignin content were designated Org(+), while those with lower contents were labeled Org(-). Both samples were obtained under similar conditions, treating SCB with ethanol at 40% v/v for 60 min, with the only difference being the temperature. Org(+) samples were treated at 160 °C, while Org(−) were treated at 200 °C. The + and – symbols in sample codes indicate higher or lower lignin contents, respectively.

*TEMPO-mediated oxidation*

TEMPO oxidation was applied to Org(+) and Org(−) samples using a TEMPO/NaBr/NaClO system (Saito et al. 2007), as evidenced in step 2 of Fig. 1. Two NaClO concentrations were evaluated (25 and 50 mmol/g substrate). In a typical experiment, 1 g of substrate (dry weight) was dispersed in 100 mL of water and incubated for 24 h (hydration step). Subsequently, 0.016 g of TEMPO and 0.1 g of NaBr were added to the dispersion and stirred until fully dissolved (*ca.* 10 min). NaClO was then added (18.6 mL of NaClO 10 wt% for 25 mmol/g substrate and 37.2 mL of NaClO 10 wt% for 50 mmol of NaClO/g substrate). The oxidation reaction was initiated upon NaClO addition, and the pH was adjusted to 10 by adding NaOH 3 mol/L dropwise. The system was stirred at 350 rpm for 130 min while maintaining the pH at $10.0 \pm 0.2$ by adding NaOH 3 mol/L as needed. After oxidation, the solid fractions were washed via centrifugation (3500 rpm, 10 min, 8 cycles) and maintained in water (solid content of ~ 0.8 wt%). The suffixes 25 and 50 were assigned to the samples oxidized with 25 and 50 mmol of NaClO/g substrate, respectively.

*Mechanical treatments*

Suspensions of oxidized pulp at ~ 0.8 wt% were homogenized using an Ultra Turrax disperser (IKA T25) at 7000 rpm for 5 min. They underwent mechanical treatment with either ultrasonication or microfluidization, as evidenced in Fig. 1 (step 3: Mechanical treatment). Oxidized samples were probe-sonicated (Eco-Sonics QR550) at 60% amplitude, 330 W, and 20 kHz for 15 min (intermittent cycles of 5 min on and 5 min off) in an ice bath, similarly to a previous report but using a shorter sonication time (Camargos and Rezende 2021). Sample Org(+)-25 was also sonicated for 30 min as a proof of concept.

For microfluidization, selected oxidized samples (Org(+)-50 and Org(−)-25, Fig. 1) were processed in a microfluidizer (M110P, Microfluidics Corp) equipped with a Z-shaped interaction chamber (200 µm inner diameter). Based on previous reports, samples passed through the system eight times (Carneiro Pessan et al. 2023). The suffixes US and MF were assigned to samples treated via ultrasonication and microfluidization, respectively.

## Characterization

*Chemical composition*

Cellulose, hemicellulose, lignin, extractives, and ash contents were determined according to the protocol of

the National Renewable Energy Laboratory (Sluiter et al. 2008). In addition, the lignin content in samples before and after TEMPO oxidation was also quantified using the acetyl bromide soluble lignin (ABSL) method (Moreira-Vilar et al. 2014).

*Percentage of fibrillation*

After ultrasonication, dispersions were diluted to 0.4 wt% to reduce viscosity and then centrifuged (3500 rpm, 10 min) to separate residual non-fibrillated fibers. The liquid fraction was separated from the precipitate (composed of non-fibrillated fibers). The solid fraction was then dried in a convection oven (105 °C) until a constant weight was reached. The percentage of fibrillation (*%Fibr*) was calculated according to Eq. 1:

$$\%Fibr = \frac{C_i \times V_i - m_{lf}}{C_i \times V_i} \times 100 \quad (1)$$

where: $C_i$ is the initial concentration of the dispersion; $V_i$ is the initial volume of the dispersion; and $m_{lf}$ is the dry mass of the large fibers.

*CNF morphology by atomic force microscopy (AFM)*

CNFs were analyzed by AFM in the non-contact mode under ambient conditions (Shimadzu, SPM-9600) using silicon tips (NCHR Pointprobe, Nanoworld) with a cantilever spring constant of 42 N/m and nominal resonance frequency of 318 kHz. Before analysis, the dispersions were diluted to 0.0025 wt%, deposited onto cleaved mica supports, and dried inside a desiccator. The diameter and length of CNFs were measured using Gwyddion 2.56 software. For each sample, 150 CNFs were measured to create diameter and length distribution histograms.

*Conductometric titration*

The content of oxidized groups ($COO^-$) of TEMPO-oxidized fibers was determined by conductometric titration following previously reported procedures (Katz et al. 1984; Foster et al. 2018).

*Substrate morphology by field emission scanning electron microscopy (FESEM)*

The morphology of the raw, pretreated, and oxidized substrates was analyzed by FESEM (FEI Quanta 250) operating at 2 kV. Dried samples were sputter-coated with iridium (Baltec, Oerlikon-Balzers) at 11.3 mV for 120 s before analysis. For oxidized samples, dispersions were freeze-dried (Terroni, LS Series) prior to analysis. At least 20 images of each sample were captured to ensure reproducibility.

*Zeta potential*

The zeta potential of CNFs dispersed at pH 5 (0.05 wt%) was measured using a Zetasizer® 300 ZS (Malvern) in backscattering (173°) mode. Each measurement was conducted in triplicate, with at least 10 scans per measurement.

*Rheology measurements*

The rheological properties of 1 wt% CNF dispersions were evaluated using a Haake MARS 60 rheometer (Thermo Fisher) equipped with parallel plate geometry (35 mm). Flow curves were obtained using a pre-shear 0.001 $s^{-1}$ for 100 s and a test from 0.001 to 1000 $s^{-1}$. Storage modulus (G') and loss modulus (G") were determined using oscillatory measurements in a strain sweep from 0.01 to 50% at 1 Hz. All measurements were performed in duplicate.

## Results and discussion

### Effect of the delignification process on the chemical composition of SCB

Delignification is the first stage in CNF preparation, facilitating subsequent surface modification and fibrillation. While cellulose-enriched substrates are conventionally used for CNF production, retaining higher levels of residual lignin represents an alternative strategy that may help reduce excessive fiber damage during CNF isolation from lignocellulosic biomass (Zhang et al. 2023).

Figure 2 shows the chemical composition of the substrates used for CNF production. Organosolv treatments reduced lignin content from 33% in raw

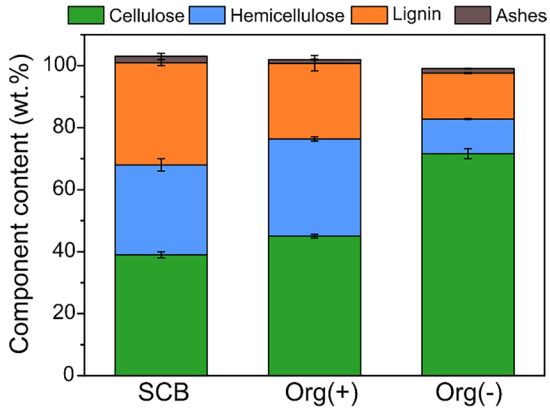


**Fig. 2** Chemical composition of the raw SCB and organosolv-treated substrates, indicating cellulose, hemicellulose, lignin, and ash contents. Error bars represent standard deviations of duplicates

SCB to 24% in Org(+) and to 15% in Org(−), the selected conditions for CNF production. Among all conditions evaluated in the DoE, the lowest lignin content achieved by organosolv treatments was 11% (Supplementary Information, Section S1), obtained under the same ethanol concentration and temperature as Org(−) (40% v/v and 200 °C), but with a reaction time of 2 h instead of 1 h. The condition shown in Fig. 1 was selected to minimize reaction time, as the objective was not to reduce the lignin content to the lowest possible value. The resulting lignin contents are consistent with previous reports on similar biomasses treated by organosolv extraction using aqueous ethanol solutions (Rabelo et al. 2022).

Organosolv extraction was selected due to its proven efficiency in removing lignin from herbaceous feedstocks, attributed to the synergistic effect of water and ethanol in hydrolyzing linkages between cellulose and lignin and in solubilizing the macromolecule after cleavage (Rabelo et al. 2022). This method offers additional advantages, including the recovery of high-purity lignin as a co-product and the potential for solvent recycling (Eraghi Kazzaz and Fatehi 2020). Despite these benefits, CNF production from organosolv-treated substrates remains relatively limited and often requires additional bleaching steps to further reduce lignin content, as reported for SCB (Pinto et al. 2019; Rabelo et al. 2022; Carneiro Pessan et al. 2023).

## CNF morphology

Following delignification, the substrates were subjected to TEMPO oxidation using two NaClO concentrations: 25 mmol/g (low) and 50 mmol/g (high), followed by ultrasonication or microfluidization to produce CNFs (Fig. 1). The morphology of the CNFs obtained by ultrasonication and microfluidization is shown in Figs. 3 and 4, respectively, along with histograms of length and diameter distributions. Overall, samples exhibited a typical CNF morphology, with structures averaging 531 to 813 nm in length, extending up to micrometers, and average diameters of approximately 1–2 nm.

The Org(+)-25-US sample exhibited a higher average length (813 nm, Fig. 3a) compared to the Org(+)-50-US (665 nm, Fig. 3b). Both samples underwent the same delignification conditions, but Org(+)-50-US was TEMPO-oxidized using a higher concentration of NaClO. This suggests that increasing the oxidizing agent concentration weakens the fibers, facilitating their fragmentation and resulting in shorter CNFs. Despite this increased average length, TEMPO oxidation using 25 mmol NaClO/g substrate yielded a fibrillation of 70 ± 2%. In contrast, when the NaClO concentration was increased to 50 mmol/g substrate, no significant amount of unfibrillated fibers were measured. It is important to note that only the nanofibrillated fraction of Org(+)-25-US was analyzed by AFM. An additional experiment was conducted by increasing sonication time from 15 to 30 min for this substrate, which did not significantly improve fibrillation yield (75 ± 3%). Instead, the average CNF length decreased from 813 to 655 nm (Supplementary Information, Section S2, Figure S2). These results suggest that longer ultrasonication primarily shortens already fibrillated CNFs rather than promoting further fibrillation of larger fiber bundles, highlighting that substrate accessibility is essential for efficient mechanical treatment. Therefore, under the tested conditions, increasing the oxidation level appears to be more effective for enhancing fibrillation than extending the mechanical treatment time.

For Org(−) samples, which had a lower initial lignin content, the average CNF lengths were 685 and 531 nm for samples treated with 25 or 50 mmol NaClO/g substrate, respectively, and no significant amount of unfibrillated fibers were measured. These average lengths also suggest that increasing oxidizing

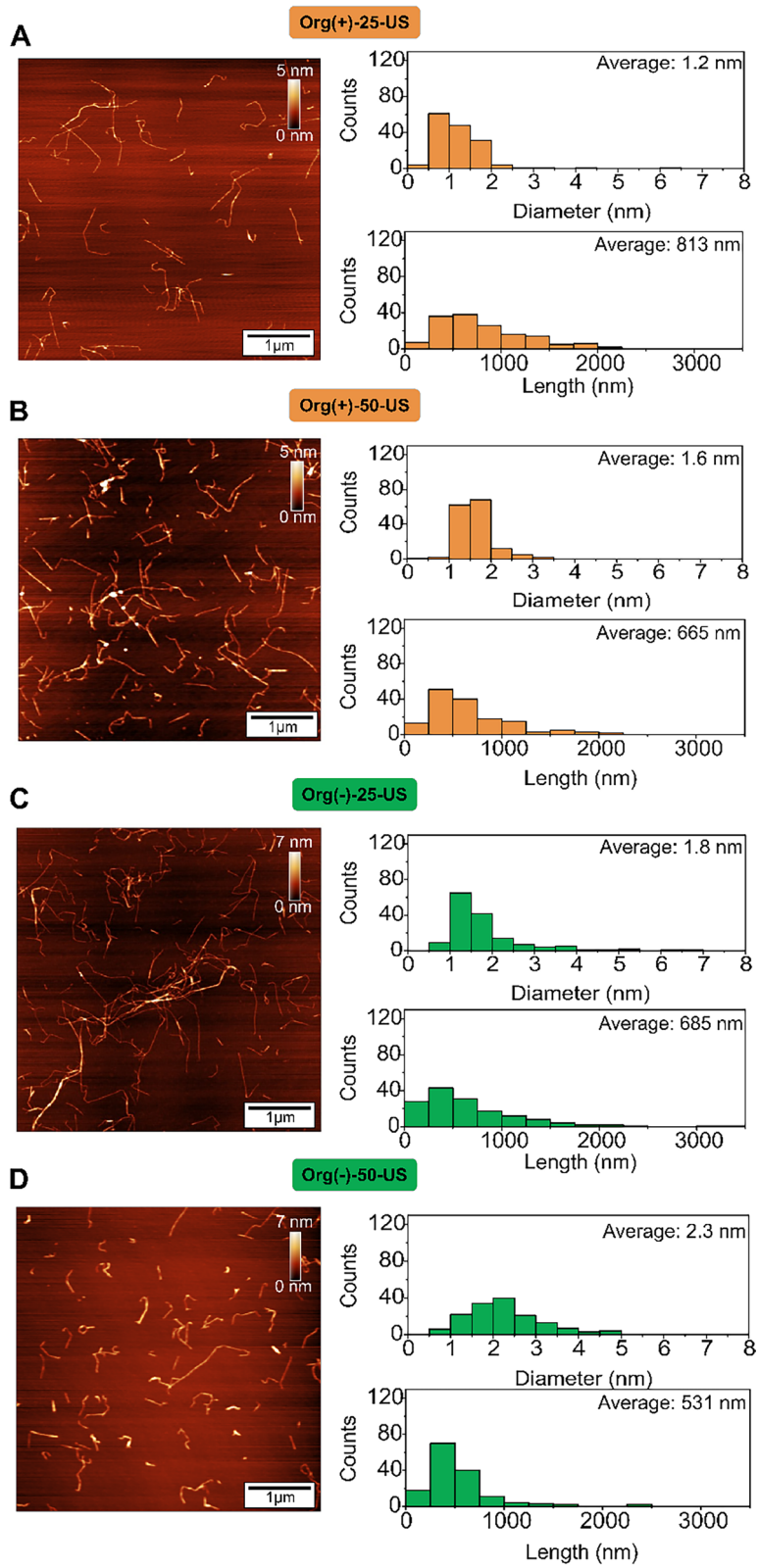


**Fig. 3** Morphology of CNFs prepared by TEMPO oxidation and ultrasonication and their respective diameter and length histograms of samples with higher initial lignin content treated with 25 mmol NaClO/g, sample Org(+)-25-US (**a**) or using 50 mmol NaClO/g, Org(+)-50-US (**b**); and of samples with lower initial lignin content treated with 25 mmol NaClO/g, sample Org(−)-25-US (**c**) or using 50 mmol NaClO/g, sample Org(−)-25-US (**d**). Histograms were obtained by measuring 150 CNFs in AFM images. Height profiles were used to determine diameters

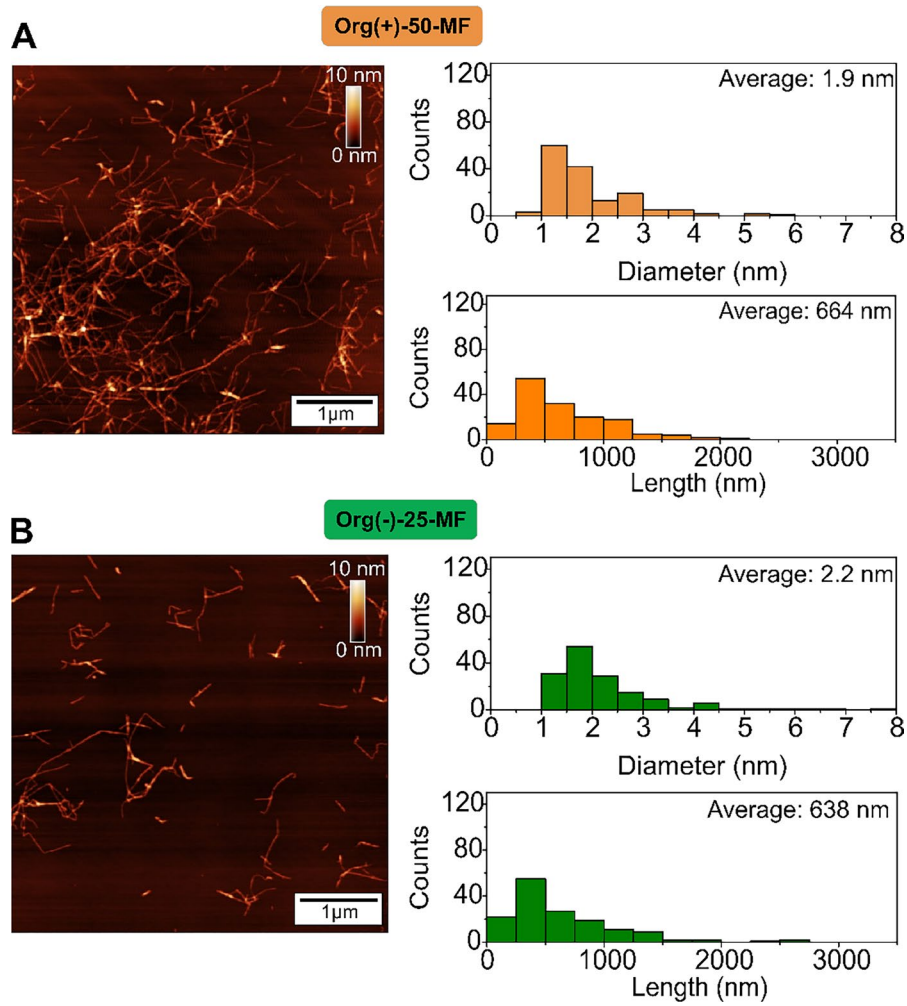


**Fig. 4** Morphology of CNFs prepared by TEMPO oxidation and microfluidization and their respective diameter and length histograms of samples with higher initial lignin content treated with 50 mmol NaClO/g, sample Org(+)-50-MF (**a**); and of samples with lower initial lignin content treated with 25 mmol NaClO/g, sample Org(−)-25-MF (**b**). Histograms were obtained by measuring 150 CNFs in AFM images. Height profiles were used to determine diameters

agent concentration reduces CNF length. When comparing substrates with different initial lignin contents oxidized with the same amount of NaClO (e.g., Org(+)-25-US vs. Org(−)-25-US or Org(+)-50-US vs. Org(−)-50-US), Org(−) samples were more easily fibrillated but yielded shorter CNFs than Org(+) samples. This indicates that greater lignin removal during the delignification step leads to the formation of shorter CNFs when the same NaClO concentration is used during TEMPO oxidation.

Figure 4 shows CNFs produced via microfluidization using the selected samples Org(+)-50 and Org(−)-25. The average diameters and lengths of CNFs produced by microfluidization were comparable to those obtained by ultrasonication, indicating that the fibrillation method had minor impact on CNF morphology under the tested conditions. It is important to note that microfluidization was performed under milder conditions to avoid extensive fiber damage, using only the chamber with the larger inner diameter (200 µm) and eight processing cycles (Carneiro Pessan et al. 2023). This comparison was carried out due to the differences in the fibrillation mechanisms between ultrasonication and microfluidization. In ultrasonication, microscopic gas bubbles are generated, expanded, and imploded, deconstructing fibers through cavitation (Hassan et al. 2018; Hoo et al. 2022). In contrast, microfluidization promotes fibrillation by forcing fibers through a narrow chamber under high pressure, promoting fibrillation (Khan et al. 2014). For both ultrasonication or microfluidization, increase the processing time or number of passes would likely reduce CNF lengths (Camargos and Rezende 2021; Carneiro Pessan et al. 2023).

It is important to note that substrates with higher lignin content typically require higher amounts of oxidizing agent compared to those with very low lignin levels (below 5 wt%), for which concentrations in the range of 5–15 mmol/g are commonly used (Xu et al. 2022). In contrast, substrates with higher lignin contents may require NaClO concentrations of approximately 50–60 mmol/g (Camargos and Rezende 2021; Sharma et al. 2025). Specifically for SCB, the comparison between 25 and 50 mmol NaClO/g was also intended to align with a previous study that used the same concentrations for SCB substrates with low lignin contents (below 5 wt%) obtained through organosolv-bleaching. In that study, applying NaClO concentrations above 25 mmol/g led to the formation of CNCs rather than CNFs (Pinto et al. 2019).

The CNF dimensions obtained from the partially delignified substrates are consistent with the values reported in literature for SCB, particularly in terms of diameter, as length is less frequently reported and is influenced by various factors, including the delignification process. Regarding diameter, recent studies have reported CNFs with average diameters around 2 nm, measured by AFM height, when using TEMPO oxidation on non-wood biomasses such as sugarcane bagasse (Mariano et al. 2014; Rossi et al. 2021; Lorevice et al. 2023) and hop stem (Kanai et al. 2022). CNFs produced from the partially delignified SCB in this study were longer than nanocelluloses produced from more processed substrates (subjected to organosolv and alkaline bleaching, then oxidized under the same conditions), which resulted in nanocelluloses with average lengths between 150 and 190 nm and were classified as CNCs (Pinto et al. 2019). Compared to TEMPO-oxidized CNFs derived from softwood thermomechanical pulp, CNFs from SCB exhibited thinner diameters and shorter lengths, likely due to the structural differences between the fibers and the lower recalcitrance of SCB relative to wood fibers (Okita et al. 2009). It is important to note that diameters measured by AFM are generally smaller than those measured by transmission electron microscopy (TEM), as previously reported, which should be considered when comparing nanocellulose dimensions (Chen et al. 2021).

## TEMPO oxidation effect on lignin content, surface charge, and substrate morphology

Based on the differences in CNF morphology and fibrillation, we investigated possible factors underlying the variations in CNF characteristics as a function of delignification type and oxidizing agent level. We analyzed lignin content, the degree of oxidation, residual mass after TEMPO oxidation, and substrate morphology.

Figure 5a shows the lignin content of substrates before and after TEMPO oxidation, quantified using the acetyl bromide soluble lignin (ABSL) method. TEMPO oxidation significantly reduced the lignin content in both Org(+) and Org(−) samples to 5–7.5%, despite their initial differences. Lignin content varied only slightly between substates oxidized with 25 or 50 mmol NaClO/g substrate, suggesting

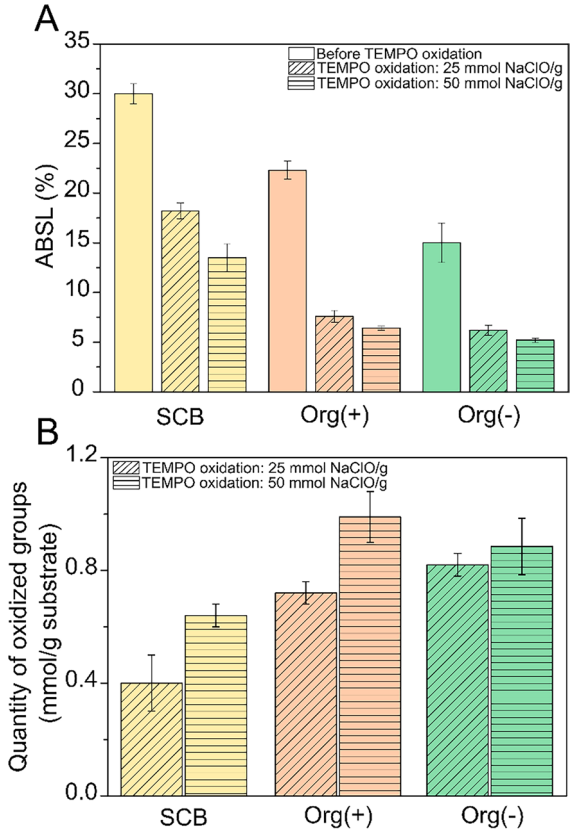


**Fig. 5** Characterization of oxidation effects: **a** ABSL quantification before and after TEMPO oxidation; **b** Quantity of oxidized groups on the fiber surface after TEMPO oxidation. Error bars represent standard deviations of duplicates

that increasing NaClO concentration did not substantially enhance lignin removal. Even when applied to raw SCB (control experiment), TEMPO oxidation reduced lignin content from 30 to 18% and 13% after 25 and 50 mmol NaClO/g substrate, respectively (Fig. 5a). This confirms that TEMPO oxidation contributes to lignin removal, as reported in previous studies (Ma et al. 2012; Rahimi et al. 2013). Therefore, it is important to evaluate the residual lignin content in CNFs derived from organosolv-treated SCB and to understand how it relates in fibrillation and morphology among the substrates.

TEMPO oxidation applied to thermomechanical pulps under similar levels of oxidizing agent has been shown to result in near-complete lignin removal (around 0.5% after oxidation), highlighting that lignin removal is influenced by substrate characteristics such as initial lignin content and fiber structure (Okita et al. 2009). Similar behavior was observed for CNFs produced from jute fibers (Sharma et al. 2025), hemp bast (Puangsin et al. 2017), and elephant grass (Camargos and Rezende 2021). In this study, the results reinforce that final lignin contents should be considered in CNF applications that seek to exploit lignin-related properties. Likewise, the findings suggest that lignin content alone does not dictate fibrillation efficiency, as indicated by the partial fibrillation observed in sample Org(+)−25 despite having a lignin content similar to that of other fully fibrillated samples.

Figure 5b shows the amount of oxidized groups ($COO^-$) on the fiber surface after TEMPO oxidation. The values ranged from 0.72 to 0.99 mmol/g substrate and can be interpreted in conjunction with the changes in lignin content. Since TEMPO oxidation contributes to lignin removal when applied to partially delignified substrates (Fig. 5a) (Ma et al. 2012; Rahimi et al. 2013), higher lignin content appears to reduce oxidation efficiency, as part of the oxidizing agent is consumed in further lignin removal rather than in cellulose modification. This effect is most evident in sample Org(+)-25, which exhibited a lower amount of $COO^-$ groups compared to the other samples, likely due to the higher lignin content in Org(+) substrates combined with the lower NaClO concentration used. Similarly, raw SCB showed lower $COO^-$ contents, of around 0.4 and 0.64 mmol/g substrate after oxidation using 25 and 50 mmol NaClO/g substrate, respectively, corroborating these findings.

The remaining mass of the substrates before and after oxidation (Support Information, Section S3, Table S2) further supports this interpretation. TEMPO-oxidized Org(+) samples retained less solid mass (59 and 39% using 25 and 50 mmol/g, respectively) than Org(−) samples (71 and 70% using 25 and 50 mmol/g, respectively). This greater mass loss in Org(+) substrates is mostly attributed to enhanced lignin removal. Moreover, considering the entire process, the final amount of CNFs produced from the same initial mass of raw SCB was comparable between samples, as discussed further.

The effects of delignification and TEMPO oxidation were also assessed by FESEM analysis (Fig. 6). Raw SCB (Fig. 6a) exhibits the typical morphology previously reported for this biomass, consisting of fibers with ~ 150 µm in diameter, composed of cellulose, hemicellulose, and lignin arranged in a compact structure (Rezende et al. 2011). The thick fibers visible in Fig. 6a correspond to conducting vessels of the sugarcane plant. These vessels are made up of thinner fibers, which become increasingly exposed in Fig. 6b and e as lignin is progressively removed by the organosolv treatment. Lignin is known to act as an adhesive within the fiber bundle. Therefore, its removal leads to fiber exposure and, eventually, complete separation of microfibers (Rezende et al. 2011).

Fiber separation resulting from TEMPO oxidation is shown in Fig. 6c, d, and f. These morphological changes strongly correlate with lignin content and play a crucial role in CNF production, alongside the presence of $COO^-$ groups. However, Org(+)-25 samples (Fig. 6c) still contained large fiber bundles after TEMPO oxidation, which likely contributed to their lower fibrillation yield. This suggests that a lower level of TEMPO oxidation was insufficient to separate fibers in lignin-rich substrates. These results also indicate that the morphological changes induced by delignification and TEMPO oxidation are key determinants of CNF yield and properties. Although tracking lignin content is important for understanding chemical modifications during TEMPO oxidation, it becomes more informative when considered alongside morphological changes.

Based on the chemical, surface, and morphological characterizations, Fig. 7 summarizes the effects of each processing step on CNF production. Starting from raw SCB, organosolv extraction produced substrates with different lignin quantities but similar

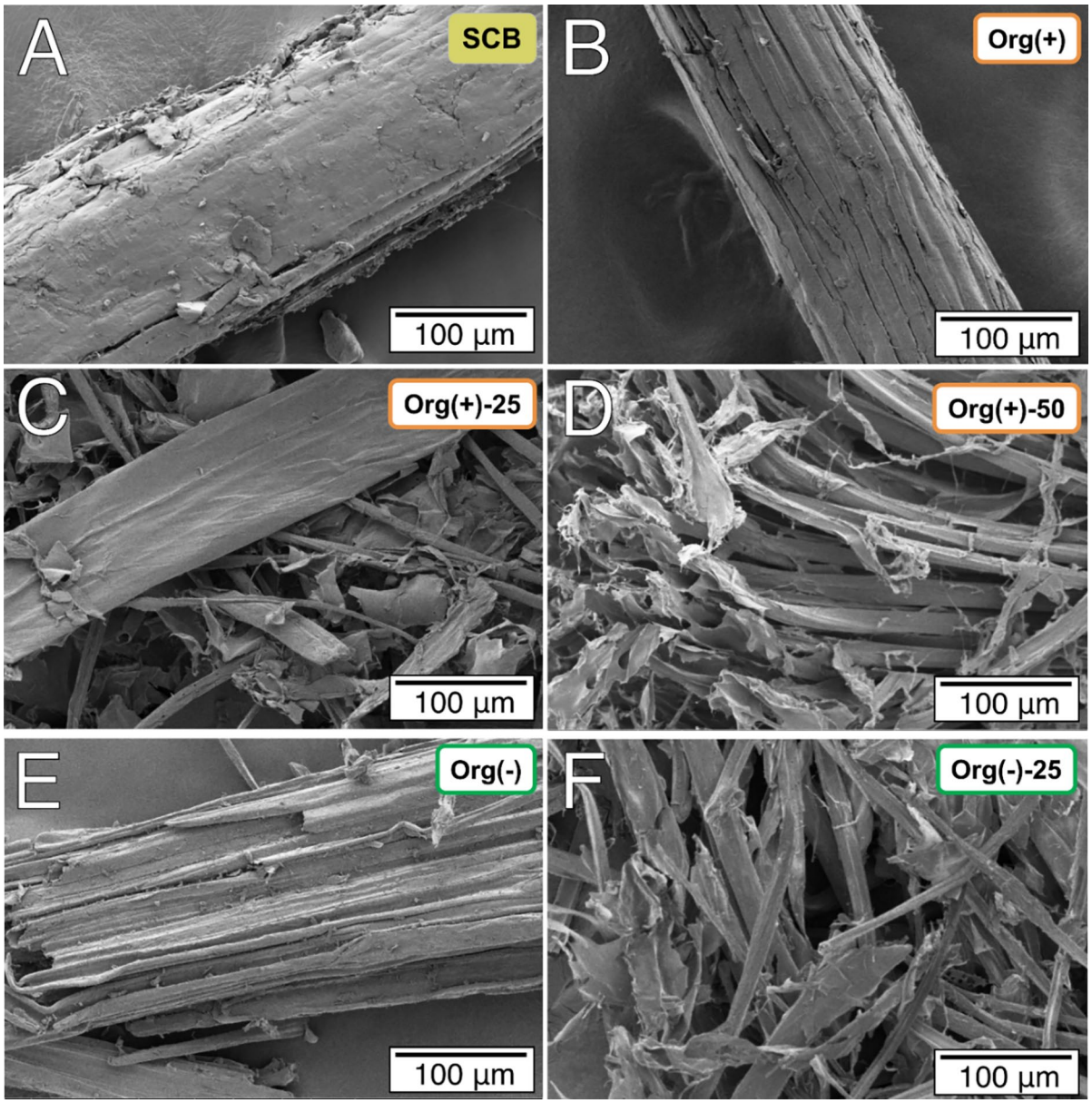


**Fig. 6** FESEM images showing SCB morphology before and after chemical treatments: raw SCB (**a**); SCB after milder delignification yielding sample Org(+) (**b**); Org(+) followed by TEMPO oxidation using 25 (**c**) or 50 mmol/g substrate (**d**); SCB after higher delignification yielding sample Org(−) (**e**); and Org(−) followed by TEMPO oxidation using 25 mmol/g substrate (**f**)

morphologies, with cellulose fibers still covered and less exposed. TEMPO oxidation played a significant role in reducing lignin content, regardless of the quantity of remaining lignin after delignification, and in modifying substrate morphology by promoting fiber separation. However, the substrate with higher initial lignin content treated using 25 mmol NaClO/g still contained microfibril bundles alongside individualized microfibrils. This condition resulted in longer CNFs on average, but the sample were less fibrillated overall. In contrast, the same substrate treated using 50 mmol NaClO/g, as well as the Org(−) samples

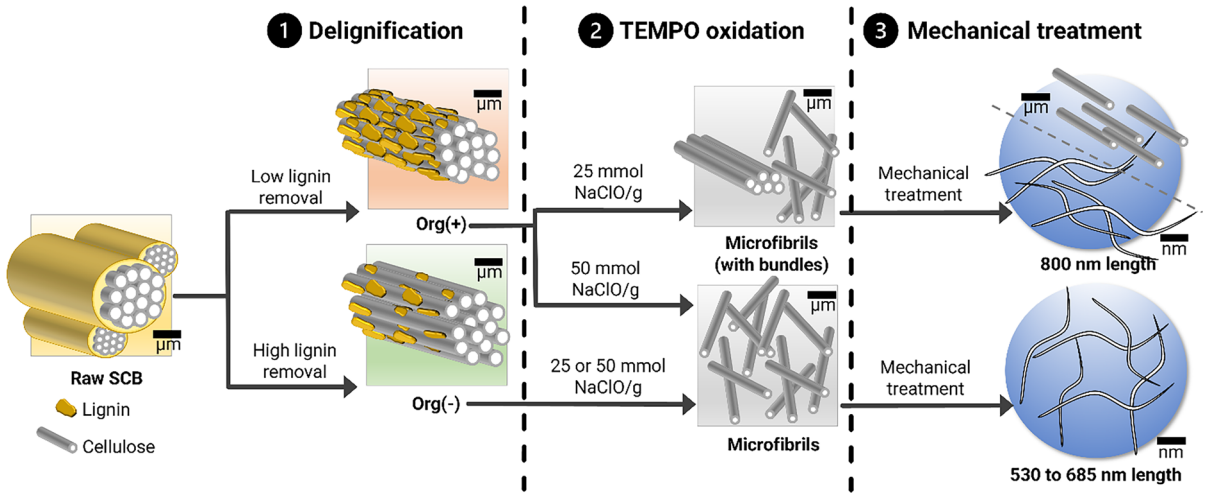


**Fig. 7** Schematic summary rationalizing the effect of each step in CNF production from SCB

treated with either 25 or 50 mmol NaClO/g, consisted primarily of individualized microfibrils prior to mechanical treatment and yielded CNFs with an average length of 530–685 nm on average and considered nearly completely fibrillated.

CNF characterization: zeta potential and rheology

The zeta potential of CNFs is a crucial parameter that governs their colloidal stability and suitability for various applications. In TEMPO-oxidized CNFs, it reflects the electrostatic repulsion arising from the carboxylated groups introduced on the fibril surface (Isogai et al. 2011). As shown in Fig. 8, all prepared CNF samples exhibit strongly negative zeta potential values, indicating good colloidal stability (Foster et al., 2018). Among the ultrasonicated samples, Org(+)-25-US presented a less negative zeta potential than Org(+)-50-US, likely due to the lower concentration of oxidized groups on the fiber surface (Fig. 5b), which are the primary contributors to electrostatic stabilization. In contrast, no significant differences were observed between Org(−)-25-US and Org(−)-50-US, probably because the Org(−), with lower initial lignin content, underwent more efficient oxidation in both cases. When comparing mechanical treatments, ultrasonicated CNFs exhibited more negative zeta potential than those prepared via microfluidization, suggesting a higher surface charge density. Literature reports values between −80 and −60 mV

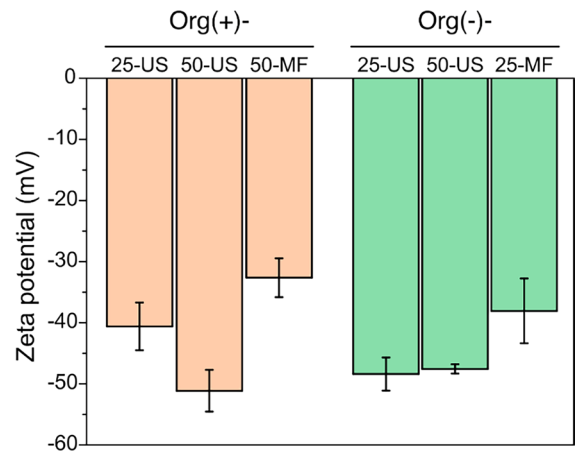


**Fig. 8** Zeta potential of the prepared CNFs at pH 5. Error bars represent standard deviations of triplicates

for TEMPO-oxidized CNFs (Isogai et al. 2011; Levanič et al. 2022), which are slightly more negative than the values observed in this work. This discrepancy may stem from the reduced carboxylate content, as part of the oxidizing agent was consumed during lignin removal.

Figure 9 displays the flow curves and images of selected CNF samples prepared via ultrasonication and microfluidization at a concentration of 1 wt%. The rheological behavior of CNFs in water is critical for applications such as gels, 3D printing, and film formation, as it influences their flow properties,

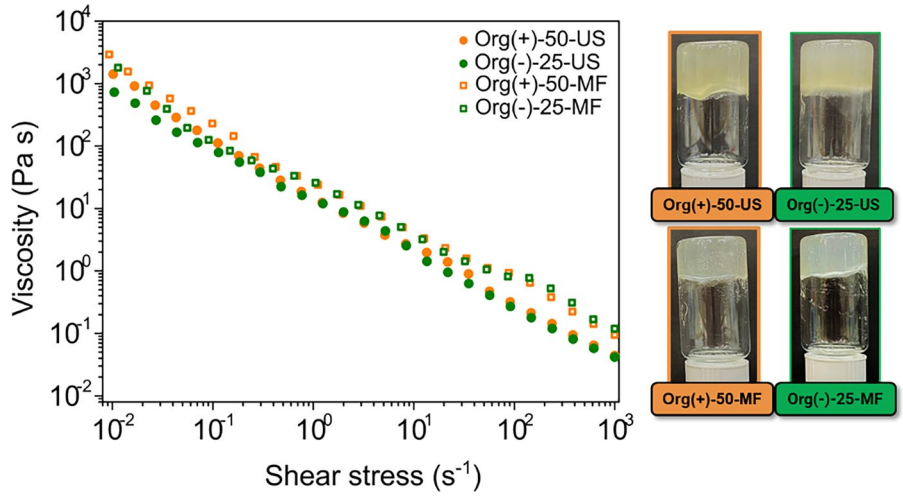


**Fig. 9** Rheology profiles and invertible gel test of samples prepared by ultrasonication

**Table 1** Process yields expressed as mass remaining after delignification, oxidation, and fibrillation starting from 100 g of raw SCB. Error represents standard deviations of duplicates

| Sample | Mass after delignification(g) | Mass after oxidation and fibrillation (g) |
|---|---|---|
| Org(+)−25 | 81 ± 4 | 33 ± 2[#] |
| Org(+)−50 | 81 ± 4 | 31 ± 4 |
| Org(−)−25 | 42 ± 4 | 30 ± 3 |
| Org(−)−50 | 42 ± 4 | 30 ± 3 |

[#]Considering 70% fibrillation yield

processability, and are an indicative of their mechanical properties. All dispersions exhibited shear-thinning behavior, a characteristic feature of CNFs in water (Bhattacharya et al. 2012; Shin and Hyun 2021; Xu et al. 2024) and behaved as invertible gels. This response suggests the formation of a percolated network due to the entanglement of flexible, elongated CNFs, reinforced by electrostatic repulsion between surface $COO^-$ groups. Furthermore, gel-like behavior was observed, as indicated by oscillatory rheology, where the storage modulus (G′) exceeded the loss modulus (G″) (Supplementary Information, Section S4, Figure S3).

## Process considerations

In addition to CNF characterization, process yield is a critical parameter for evaluating the efficiency and scalability of the production route. Table 1 summarizes process yields, including the residual mass after delignification, as well as the yields following TEMPO-mediated oxidation and mechanical fibrillation. The total amount of CNFs obtained from 100 g of raw SCB was comparable among all samples, ranging from 30 to 33 g. These values indicate that, regardless of the processing route, the overall CNF yield remained relatively consistent. However, the distribution of mass loss varied across the different processing stages, depending on the delignification strategy and oxidation conditions applied.

The first notable difference was observed in the mass retained after delignification. The Org(+) substrates, which underwent delignification at 160 °C, retained a higher amount of solid material, yielding 81 g per 100 g of raw SCB. In contrast, Org(−) substrates, treated at a higher temperature (200 °C), retained only 42 g per 100 g of raw SCB. This observation is consistent with the greater lignin solubilization efficiency of organosolv at elevated temperatures (Rabelo et al. 2022) and aligns with results from the DoE. As expected, the mass loss during TEMPO oxidation showed the opposite trend. The Org(+) samples experienced greater mass loss during oxidation compared to the Org(−) ones. As previously discussed, TEMPO oxidation functions as a secondary delignification step, which explains the increased higher mass loss for samples with higher lignin content.

Despite the similar overall CNF yields, the most effective processing strategy should account for additional factors such as CNF-fiber bundle separation, lignin recovery potential, and energy

efficiency. One key aspect is fibrillation efficiency. The Org(+)−25-US sample exhibited a lower fibrillation yield (70%), as a significant fraction of the oxidized substrate remained as larger fiber bundles. This suggest that additional separation steps, such as centrifugation or filtration, may be necessary to isolate the nano-sized fraction (Masruchin et al. 2015). However, such fractionation steps can increase processing costs and must be carefully considered in biomass valorization strategies. Alternatively, retaining both nano- and micro-scale fibers in the final material may be beneficial for applications that require structured hierarchical reinforcement (Ferreira and Rezende 2018). This approach can improve global yield by incorporating both oxidized fibers and fibrillated nanocellulose into the final product. Indeed, even in substrates that undergo nearly complete fibrillation, residual micrometer-scale fibers may still be present due to the inherent heterogeneity of lignocellulosic materials. Depending on the target application, these residual fibers may need to be removed through post-processing steps.

Another critical aspect is the potential for lignin recovery, which is highly relevant for biorefinery strategies. The organosolv process yields sulfur-free lignin, which is attractive to produce materials and chemicals (Rabelo et al. 2022). The organosolv treatment that generated the Org(−) samples removed a greater quantity of lignin during delignification, facilitating its recovery and enhancing the circularity of biomass processing. In contrast, Org(+) substrates retained more lignin initially, but the macromolecule was subsequently oxidized during the TEMPO oxidation step, reducing the feasibility of recovering pure lignin as a valuable co-product. In this case, a trade-off between delignification temperature and lignin recovery must be considered.

A final consideration is the trade-off between delignification severity and oxidation intensity. The milder delignification used to produce Org(+) samples required less energy (temperature of 160 °C) compared to the more severe delignification used for Org(−) samples (temperature of 200 °C). However, Org(+) samples required higher concentrations of oxidizing agent than Org(−) to achieve nearly complete fibrillation. Since the final CNF yields and properties were comparable, the most cost-effective strategy will depend on whether minimizing energy consumption during delignification or reducing chemical consumption during oxidation is prioritized. Additionally, the findings reported here suggest that intermediate NaClO concentrations could be explored, potentially between 25 and 50 mmol/g for Org(+) and between 5 and 25 mmol/g for Org(−).

## Conclusion

This study elucidated the impact of producing CNFs from partially delignified SCB, focusing on the relationship between substrate properties (lignin content, oxidation efficiency, and fiber morphology) and the resulting CNF characteristics. Although final CNF yields were similar across conditions (30–33 g per 100 g of raw SCB), the distribution of mass losses varied depending on the delignification and TEMPO oxidation steps, which should be considered for co-product recovery strategies. Retaining more lignin and applying 25 mmol NaClO/g substrate resulted in longer CNFs but incomplete fibrillation, ultimately requiring higher oxidizing agent concentrations to increase fibrillation, despite resulting in shorter fibrils. In contrast, substrates with lower lignin content enabled the use of lower oxidizing agent concentrations. CNF morphology was primarily governed by the combined chemical and structural changes induced by the sequence of delignification and TEMPO oxidation. These findings demonstrate the feasibility of producing CNFs via a single delignification step, thereby simplifying the process. The resulting CNFs exhibit promising characteristics for applications such as hydrogels, films, mechanical reinforcement, and rheology modifiers. Furthermore, this work contributes to the strategic valorization of sugarcane bagasse, providing an efficient pathway for converting agricultural residues into high-value nanomaterials.

**Acknowledgements** The authors thank Dr. Juliana da Silva Bernardes (LNNano/CNPEM) for microfluidizer access; Dr. Fernando Galembeck for AFM access; and Dr. Edvaldo Sabadini and Fernando Bonin Okasaki for rheology measurements. We thank the LIMicro-IQ – Microscopy Core Facility (RRID:SCR_024633) at the Universidade Estadual de Campinas for support. The Quanta FEG 250 system was partially funded by a FAPESP grant #23/01620-4 for the LIMicro-IQ Core Facility.

**Author contributions** ES: Conceptualization, Data curation, Formal analysis, Investigation, Methodology, Validation,

Visualization, Writing—original draft, Writing—review and editing. LOP: Data curation, Formal analysis, Investigation, Methodology, Validation, Visualization, Writing—original draft, Writing—review and editing. CAR: Conceptualization, Formal analysis, Funding acquisition, Investigation, Methodology, Project administration, Resources, Supervision, Visualization, Writing—original draft, Writing—review and editing.

**Funding** This work was supported by São Paulo Research Foundation (grants number 15/13684-0, 19/19360–3, 21/12071-6, 23/01620–4); Conselho Nacional de Desenvolvimento Científico e Tecnológico (142570/2019-2), and financed in part by the Coordenação de Aperfeiçoamento de Pessoal de Nível Superior—Brasil (CAPES)—Finance Code 001.

**Data availability** Data can be made available upon request to the corresponding author.

**Declarations**

**Conflict of interest** The authors declare no competing interests.

## References

Abitbol T, Rivkin A, Cao Y, Nevo T, Abraham E, Ben-Shalom T, Lapidot S, Shoseyov O (2016) Nanocellulose, a tiny fiber with huge applications. Curr Opin Biotechnol 39:76–88. https://doi.org/10.1016/j.copbio.2016.01.002

Almeida RO, Ramos A, Kimiaei E, Österberg M, Maloney TC, Gamelas JAF (2024) Improvement of the properties of nanocellulose suspensions and films by the presence of residual lignin. Cellulose 31:10951–10967. https://doi.org/10.1007/s10570-024-06222-y

Bhattacharya M, Malinen MM, Lauren P, Lou YR, Kuisma SW, Kanninen L, Lille M, Corlu A, GuGuen-Guillouzo C, Ikkala O, Laukkanen A, Urtti A, Yliperttula M (2012) Nanofibrillar cellulose hydrogel promotes three-dimensional liver cell culture. J Controlled Release 164:291–298. https://doi.org/10.1016/j.jconrel.2012.06.039

Camargos CHM, Rezende CA (2021) Structure-property relationships of cellulose nanocrystals and nanofibrils: implications for the design and performance of nanocomposites and all-nanocellulose systems. ACS Appl Nano Mater 4:10505–10518. https://doi.org/10.1021/acsanm.1c02008

Carneiro Pessan C, Silva Bernardes J, Bettini SHP, Leite ER (2023) Oxidized cellulose nanofibers from sugarcane bagasse obtained by microfluidization: morphology and rheological behavior. Carbohydr Polym 304:120505. https://doi.org/10.1016/j.carbpol.2022.120505

Chen M, Parot J, Hackley VA, Zou S, Johnston LJ (2021) Afm characterization of cellulose nanocrystal height and width using internal calibration standards. Cellulose 28:1933–1946. https://doi.org/10.1007/s10570-021-03678-0

de Amorim JDP, de Souza KC, Duarte CR, Ribeiro FAS, Silva GS, de Farias PMA, Stingl A, Costa AFS, Vinhas GM, Sarubbo LA (2020) Plant and bacterial nanocellulose: production, properties and applications in medicine, food, cosmetics, electronics and engineering. A Review Environ Chem Lett 18:851–869. https://doi.org/10.1007/s10311-020-00989-9

de Oliveira FB, Bras J, Borges Pimenta MT, Curvelo AAS, Balgacem MN (2016) Production of cellulose nanocrystals from sugarcane bagasse fibers and pith. Ind Crops Prod 93:48–57. https://doi.org/10.1016/j.indcrop.2016.04.064

De France KJ, Hoare T, Cranston ED (2017) Review of hydrogels and aerogels containing nanocellulose. Chem Mater 29:4609–4631. https://doi.org/10.1021/acs.chemmater.7b00531

Du H, Liu W, Zhang M, Si C, Zhang X, Li B (2019) Cellulose nanocrystals and cellulose nanofibrils based hydrogels for biomedical applications. Carbohydr Polym 209:130–144. https://doi.org/10.1016/j.carbpol.2019.01.020

Eichhorn SJ, Dufresne A, Aranguren M, Marcovich NE, Capadona JR, Rowan SJ, Weder C, Thielemans W, Roman M, Renneckar S, Gindl W, Veigel S, Keckes J, Yano H, Abe K, Nogi M, Nakagaito AN, Mangalam A, Simonsen J, Benight AS, Bismarck A, Berglund LA, Peijs T (2010) Review: current international research into cellulose nanofibres and nanocomposites. J Mater Sci 45:1–33. https://doi.org/10.1007/s10853-009-3874-0

Eraghi Kazzaz A, Fatehi P (2020) Technical lignin and its potential modification routes: a mini-review. Ind Crops Prod 154:112732. https://doi.org/10.1016/j.indcrop.2020.112732

Fang Z, Hou G, Chen C, Hu L (2019) Nanocellulose-based films and their emerging applications. Curr Opin Solid State Mater Sci 23:100764. https://doi.org/10.1016/j.cossms.2019.07.003

Ferreira ES, Rezende CA (2018) Simple preparation of cellulosic lightweight materials from Eucalyptus pulp. ACS Sustain Chem Eng 6:14365–14373. https://doi.org/10.1021/acssuschemeng.8b03071

Ferreira ES, Rezende CA, Cranston ED (2021) Fundamentals of cellulose lightweight materials: bio-based assemblies with tailored properties. Green Chem 23:3542–3568. https://doi.org/10.1039/D1GC00326G

Han X, Bi R, Oguzlu H, Takada M, Jiang J, Jiang F, Bao J, Saddler JN (2020) Potential to produce sugars and lignin-containing cellulose nanofibrils from enzymatically hydrolyzed chemi-thermomechanical pulps. ACS Sustain Chem Eng 8:14955–14963. https://doi.org/10.1021/acssuschemeng.0c05183

Haroni S, Zaki Dizaji H, Bahrami H, González Alriols M (2021) Sustainable production of cellulose nanofiber from sugarcane trash: a quality and life cycle assessment. Ind Crops Prod 173:114084. https://doi.org/10.1016/j.indcrop.2021.114084

Hassan SS, Williams GA, Jaiswal AK (2018) Emerging technologies for the pretreatment of lignocellulosic biomass. Bioresour Technol 262:310–318. https://doi.org/10.1016/j.biortech.2018.04.099

Himmel ME, Ding S-Y, Johnson DK, Adney WS, Nimlos MR, Brady JW, Foust TD (2007) Biomass recalcitrance: engineering plants and enzymes for biofuels production. Science 315:804–807. https://doi.org/10.1126/science.1137016

Hoeng F, Denneulin A, Bras J (2016) Use of nanocellulose in printed electronics: a review. Nanoscale 8:13131–13154. https://doi.org/10.1039/C6NR03054H

Hoo DY, Low ZL, Low DYS, Tang SY, Manickam S, Tan KW, Ban ZH (2022) Ultrasonic cavitation: an effective cleaner and greener intensification technology in the extraction and surface modification of nanocellulose. Ultrason Sonochem 90:106176. https://doi.org/10.1016/j.ultsonch.2022.106176

Imani M, Ghasemian A, Dehghani-Firouzabadi MR, Afra E, Gane PAC, Rojas OJ (2019) Nano-lignocellulose from recycled fibres in coatings from aqueous and ethanolic media: effect of residual lignin on wetting and offset printing quality. Nord Pulp Pap Res J 34:200–210. https://doi.org/10.1515/npprj-2018-0053

Isogai A, Saito T, Fukuzumi H (2011) TEMPO-oxidized cellulose nanofibers. Nanoscale 3:71–85. https://doi.org/10.1039/C0NR00583E

Iwamoto S, Nakagaito AN, Yano H (2007) Nano-fibrillation of pulp fibers for the processing of transparent nanocomposites. Appl Phys A 89:461–466. https://doi.org/10.1007/s00339-007-4175-6

Johan Foster E, J. Moon R, P. Agarwal U, Bortner MJ, Bras J, Camarero-Espinosa S, Chan KJ, Clift MJD, Cranston ED, Eichhorn SJ, Fox DM, Hamad WY, Heux L, Jean B, Korey M, Nieh W, Ong KJ, Reid MS, Renneckar S, Roberts R, Shatkin JA, Simonsen J, Stingson-Bagby K, Wanasekara N, Youngblood J (2018) Current characterization methods for cellulose nanomaterials. Chem Soc Rev 47:2609–2679. https://doi.org/10.1039/C6CS00895J

Kanai N, Sakai T, Yamada K, Kumagai S, Kawamura I (2022) Using cellulose nanofibers isolated from waste hop stems to stabilize dodecane or olive oil-in-water pickering emulsions. Colloids Surf Physicochem Eng Asp 653:129956. https://doi.org/10.1016/j.colsurfa.2022.129956

Kargupta W, Seifert R, Martinez M, Olson J, Tanner J, Batchelor W (2021) Sustainable production process of mechanically prepared nanocellulose from hardwood and softwood: a comparative investigation of refining energy consumption at laboratory and pilot scale. Ind Crops Prod 171:113868. https://doi.org/10.1016/j.indcrop.2021.113868

Katz S, Beatson R, Anthony M (1984) The determination of strong and weak acidic groups in sulfite pulps. undefined

Kedzior SA, Gabriel VA, Dubé MA, Cranston ED (2021) Nanocellulose in Emulsions and Heterogeneous Water-Based Polymer Systems: A Review. Adv Mater 33:2002404. https://doi.org/10.1002/adma.202002404

Khan A, Vu KD, Chauve G, Bouchard J, Riedl B, Lacroix M (2014) Optimization of microfluidization for the homogeneous distribution of cellulose nanocrystals (CNCs) in biopolymeric matrix. Cellulose 21:3457–3468. https://doi.org/10.1007/s10570-014-0361-9

Levanič J, Svedström K, Liljeström V, Šernek M, Črnivec IGO, Ulrih NP, Haapala A (2022) Cellulose fiber and nanofibril characteristics in a continuous sono-assisted process for production of TEMPO-oxidized nanofibrillated cellulose. Cellulose 29:9121–9142. https://doi.org/10.1007/s10570-022-04845-7

Lorevice MV, Claro PIC, Aleixo NA, Martins LS, Maia MT, Oliveira APS, Martinez DST, Gouveia RF (2023) Designing 3d fractal morphology of eco-friendly nanocellulose-based composite aerogels for water remediation. Chem Eng J 462:142166. https://doi.org/10.1016/j.cej.2023.142166

Ma P, Fu S, Zhai H, Law K, Daneault C (2012) Influence of TEMPO-mediated oxidation on the lignin of thermomechanical pulp. Bioresour Technol 118:607–610. https://doi.org/10.1016/j.biortech.2012.05.037

Mariano M, El Kissi N, Dufresne A (2014) Cellulose nanocrystals and related nanocomposites: review of some properties and challenges. J Polym Sci Part B Polym Phys 52:791–806. https://doi.org/10.1002/polb.23490

Masruchin N, Park B-D, Causin V, Um IC (2015) Characteristics of TEMPO-oxidized cellulose fibril-based hydrogels induced by cationic ions and their properties. Cellulose 22:1993–2010. https://doi.org/10.1007/s10570-015-0624-0

Moon RJ, Martini A, Nairn J, Simonsen J, Youngblood J (2011) Cellulose nanomaterials review: structure, properties and nanocomposites. Chem Soc Rev 40:3941–3994. https://doi.org/10.1039/C0CS00108B

Moreira-Vilar FC, Siqueira-Soares R de C, Finger-Teixeira A, de Oliveira DM, Ferro, AP, da Rocha GJ, Ferrarese MLL, dos Santos WD, Ferrarese-Filho O (2014) The Acetyl Bromide Method Is Faster, Simpler and Presents Best Recovery of Lignin in Different Herbaceous Tissues than Klason and Thioglycolic Acid Methods. PLOS ONE 9:e110000. https://doi.org/10.1371/journal.pone.0110000

Okita Y, Saito T, Isogai A (2009) TEMPO-mediated oxidation of softwood thermomechanical pulp. Hfsg 63:529–535. https://doi.org/10.1515/HF.2009.096

Patterson GD, Orts WJ, McManus JD, Hsieh Y-L (2023) Cellulose and lignocellulose nanofibrils and amphiphilic and wet-resilient aerogels with concurrent sugar extraction from almond hulls. ACS Agric Sci Technol 3:140–151. https://doi.org/10.1021/acsagscitech.2c00264

Pinto LO, Bernardes JS, Rezende CA (2019) Low-energy preparation of cellulose nanofibers from sugarcane bagasse by modulating the surface charge density. Carbohydr Polym 218:145–153. https://doi.org/10.1016/j.carbpol.2019.04.070

Puangsin B, Soeta H, Saito T, Isogai A (2017) Characterization of cellulose nanofibrils prepared by direct TEMPO-mediated oxidation of hemp bast. Cellulose 24:3767–3775. https://doi.org/10.1007/s10570-017-1390-y

Rabelo SC, Nakasu PYS, Scopel E, Araújo MF, Cardoso LF, da Costa AC (2022) Organosolv Pretreatment for Biorefineries: Current Status, Perspectives, and Challenges. Bioresour Technol 128331. https://doi.org/10.1016/j.biortech.2022.128331

Rahimi A, Azarpira A, Kim H, Ralph J, Stahl SS (2013) Chemoselective metal-free aerobic alcohol oxidation in lignin. J Am Chem Soc 135:6415–6418. https://doi.org/10.1021/ja401793n

Rezende CA, de Lima MA, Maziero P, deAzevedo ER, Garcia W, Polikarpov I (2011) Chemical and morphological characterization of sugarcane bagasse submitted to a delignification process for enhanced enzymatic digestibility. Biotechnol Biofuels 4:54. https://doi.org/10.1186/1754-6834-4-54

Rol F, Saini S, Meyer V, Petit-Conil M, Bras J (2019) Production of cationic nanofibrils of cellulose by twin-screw extrusion. Ind Crops Prod 137:81–88. https://doi.org/10.1016/j.indcrop.2019.04.031

Rossi BR, Pellegrini VOA, Cortez AA, Chiromito EMS, Carvalho AJF, Pinto LO, Rezende CA, Mastelaro VR, Polikarpov I (2021) Cellulose nanofibers production using a set of recombinant enzymes. Carbohydr Polym 256:117510. https://doi.org/10.1016/j.carbpol.2020.117510

Saito T, Kimura S, Nishiyama Y, Isogai A (2007) Cellulose nanofibers prepared by TEMPO-mediated oxidation of native cellulose. Biomacromol 8:2485–2491. https://doi.org/10.1021/bm0703970

Scopel E, Camargos CHM, Pinto LO, Trevisan H, Ferreira ES, Rezende CA (2023) Broadening the product portfolio with cellulose and lignin nanoparticles in an elephant grass biorefinery. Biofuels Bioprod Biorefin 17:859–872. https://doi.org/10.1002/bbb.2476

Sharma P, Hicks S, Ruggiero AR, Sharma SK, Hsiao BS, Springstead J (2025) Extraction and analysis of carboxycellulose nanofibers from virgin plant fibers using updated TEMPO-mediated oxidation. Cellulose 32:887–902. https://doi.org/10.1007/s10570-024-06328-3

Shin S, Hyun J (2021) Rheological properties of cellulose nanofiber hydrogel for high-fidelity 3D printing. Carbohydr Polym 263:117976. https://doi.org/10.1016/j.carbpol.2021.117976

Sluiter A, Hames B, Ruiz R, Scarlata C, Sluiter J, Templeton D, Crocker D (2008) Determination of Structural Carbohydrates and Lignin in Biomass. Determ Struct Carbohydr Lignin Biomass

Sun Y, Zhang H, Li Q, Vardhanabhuti B, Wan C (2022) High lignin-containing nanocelluloses prepared via TEMPO-mediated oxidation and polyethylenimine functionalization for antioxidant and antibacterial applications. RSC Adv 12:30030–30040. https://doi.org/10.1039/D2RA04152A

Wang H, Zuo M, Ding N, Yan G, Zeng X, Tang X, Sun Y, Lei T, Lin L (2019) Preparation of nanocellulose with high-pressure homogenization from pretreated biomass with cooking with active oxygen and solid alkali. ACS Sustain Chem Eng 7:9378–9386. https://doi.org/10.1021/acssuschemeng.9b00582

Wen Y, Yuan Z, Liu X, Qu J, Yang S, Wang A, Wang C, Wei B, Xu J, Ni Y (2019) Preparation and characterization of lignin-containing cellulose nanofibril from poplar high-yield pulp via TEMPO-mediated oxidation and homogenization. ACS Sustain Chem Eng 7:6131–6139. https://doi.org/10.1021/acssuschemeng.8b06355

Xu H, Sanchez-Salvador JL, Balea A, Blanco A, Negro C (2022) Optimization of reagent consumption in TEMPO-mediated oxidation of Eucalyptus cellulose to obtain cellulose nanofibers. Cellulose 29:6611–6627. https://doi.org/10.1007/s10570-022-04672-w

Xu J, Wang P, Yuan B, Zhang H (2024) Rheology of cellulose nanocrystal and nanofibril suspensions. Carbohydr Polym 324:121527. https://doi.org/10.1016/j.carbpol.2023.121527

Zhang X, Zhang L, Fan Y, Wang Z (2023) The case-dependent lignin role in lignocellulose nanofibers preparation and functional application-a review. Green Energy Environ 8:1553–1566. https://doi.org/10.1016/j.gee.2022.09.008